European Journal of Chemistry 9 (4) (2018) 338-346

European Journal of Chemistry

Check for updates

View Journal Online
View Article Online

Selective colorimetric molecular probe for cyanide ion detection in aqueous solution

Yousef Mohammad Hijji [1,*], Hani Darwish Tabba [1], Rajeesha Rajan [1],
Hamzeh Mohammad Abdel-Halim [2], Musa Ibrahim El-Barghouthi [2] and Hutaf Mustafa Baker [3]

[1] *Department of Chemistry and Earth Sciences, Qatar University, Doha, 2713, Qatar*
yousef.hijji@qu.edu.qa (Y.M.H.), tabbah@qu.edu.qa (H.D.T.), rajeesha.rajan@qu.edu.qa (R.R.)
[2] *Department of Chemistry, The Hashemite University, Zarqa 13133, Jordan*
hamzehah@hu.edu.jo (H.M.A.H.), musab@hu.edu.jo (M.I.E.B.)
[3] *Department of Chemistry, Al Al-Bayt University, Mafraq 25113, Jordan*
hutafb@aabu.edu.jo (H.M.B.)

* *Corresponding author at: Department of Chemistry and Earth Sciences, Qatar University, Doha, 2713, Qatar.*
Tel: +974.44036548 Fax: +974.44034501 e-mail: yousef.hijji@qu.edu.qa (Y.M. Hijji).

RESEARCH ARTICLE

10.5155/eurjchem.9.4.338-346.1777

Received: 28 July 2018
Received in revised form: 08 September 2018
Accepted: 12 September 2018
Published online: 31 December 2018
Printed: 31 December 2018

KEYWORDS

DFT
Cyanide
Cyanohydrin
UV-vis spectroscopy
Visual molecular probe
5-Nitro-2-hydroxybenzaldehyde

ABSTRACT

5-Nitro-2-hydroxybenzaldehyde (1) demonstrated to be a sensitive, and a selective molecular probe for cyanide ion (CN^{-}) in aqueous media. In acetonitrile, compound 1 shows sensitivity and selectivity for cyanide, acetate and fluoride, in comparison to other investigated anions using both visual and spectroscopic means. In aqueous solution, the color becomes intense yellow upon addition of cyanide, while acetate showed this effect to a much lower extent. Significant spectral changes were also detected with the appearance of two new absorption bands at 358 and 387 nm. This was accompanied by concomitant intensity decrease for the band at 314 nm. Fluoride, dihydrogen phosphate, chloride, bromide, perchlorate, and azide showed negligible color and spectral changes for the probe in aqueous solutions. On the other hand, hydrogen sulfate caused fainting of the yellow color and gave a spectrum similar to that of the sensor in polar aprotic solvents. The cyanide ion was detected at micro molar levels in aqueous solutions with a stoichiometry of 1:1 for CN: probe in acetonitrile as the solvent. Cyanide, hydroxide, acetate, fluoride and dihydrogen phosphate showed identical changes to color and spectra, indicating a hydrogen bonding and a deprotonation mechanism.

Cite this: *Eur. J. Chem.* **2018**, *9(4)*, 338-346 **Journal website**: www.eurjchem.com

1. Introduction

Anions play an important role in biological and chemical processes. They have important impact and applications in medicine, pharmacy, biology, material science, and chemical industry. For example, fluoride is used in treating osteoporosis, dental caries and water fluoridation. Other anions such as acetates and phosphates are important in many biological reactions. In spite of all its advantages, fluoride has side effects at high concentrations such as being toxic and can cause cancer. It is poisonous and a by-product from hydrolysis of the nerve gas, sarin [1]. The development of selective and sensitive anions sensors is of high interest to researchers in many fields for selective monitoring, determination and evaluation. Colorimetric and fluorimetric anion probes have been targeted for being sensitive, low cost methods of detection. A number of reviews and reports in this field were published recently [2-11].

Cyanide, as one of the most hazardous chemical in the environment, presents a danger to human health [12]. It is known to be fatal at levels 20-25 μM and the highest allowed concentration of cyanide in drinking water should be lower than 1.9 μM. Exposure to cyanide in the environment comes from its use for production of organic chemicals such as nylon and acrylic plastics, electroplating, metal processing, photographic applications, cyanide fishing, automobile exhausts, and natural sources. Cyanide is present at low levels in insects, plants including vegetables, fruits' seeds, and nuts. It is a natural protection tool for these species from predators. Cyanide is also a hydrolysis product of the nerve gas warfare tabun [13]. Consequently, there is an urgent demand for the development of an efficient, selective, and sensitive methods for cyanide detection and monitoring in aqueous systems, soil, and air, in addition to its possible use in forensics [14].

There have been many advancements in the field of cyanide detection, and a number of cyanide sensors have been developed [15].

ISSN 2153-2249 (Print) / ISSN 2153-2257 (Online)
http://dx.doi.org/10.5155/eurjchem.9.4.338-346.1777

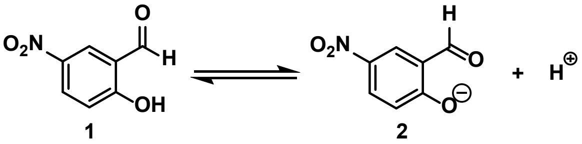

Scheme 1. Dissociation of compound **1** in polar solvents.

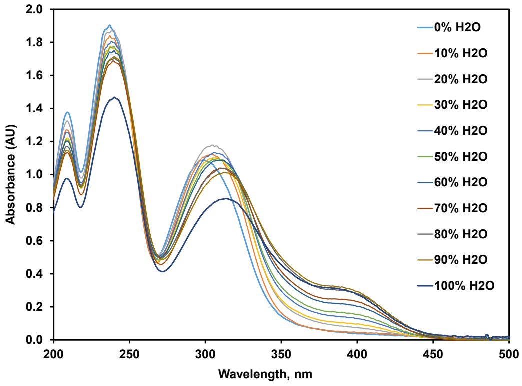

Figure 1. UV-Vis spectra of compound **1** in water, acetonitrile, and a mixture water:acetonitrile (1:9, *v*:*v*).

The sensing mechanism is based on either hydrogen bonding or chemodosimetry. For the hydrogen bonding mechanism a number of receptor moieties were investigated such as phenol [16], urea, thiourea [17], amides [5], Schiff bases [4,18-20], squarylium ions [21] and many more are continuously developing [22].

In terms of chemodosimetry approach for detection of cyanide, the nucleophilic reactivity of cyanide is utilized to gain specificity [23]. These reactions are demonstrated in displacement at metals; copper [24-27], boron [28], cobalt [10,29] and iron [30]. Addition reaction like conjugate addition to enone [26,31] by Michael-type addition [32-34], addition to aldehydes [22,28,35-37], ketones [38-40], amides [4,41,42], iminium ions [23,43-46] and thiourea [47,48]. Many of these methods exhibited limitations of poor selectivity and incompatibility in aqueous solutions. Most of these sensors have been used in organic solvent but do not work well in aqueous system. Few of these sensors were done in binary aqueous system [20,49, 50]. Among these sensors are coumarin derivatives [51] and acridinium salts [52]. None of these sensors is very soluble in water [53], therefore, an organic co-solvent had to be employed. Introducing a sensor that is soluble in water and the detection is not diminished by purely aqueous medium is still a challenging task. In the present work, we are presenting, 5-nitro-2-hydroxybenzaldehyde (**1**), as a selective and sensitive cyanide ion probe in water and in acetonitrile.

2. Experimental

5-Nitro-2-hydroxybenzaldehyde (**1**) was purchased from Aldrich and used without any further treatment. NMR data were recorded on Bruker Avance 400 MHz spectrometer in deuteriated solvents. Titrations were performed in HPLC grade acetonitrile or deionized water. UV-vis spectra were recorded on Cary 50 in quartz cuvettes. Compound **1** stock solution (1.0×10^{-3} M) was made in water. For higher concentrations it was dissolved in 1 mL of ethanol first then diluted with deionized water to the desired volume. Stock solutions (1.0×10^{-2} M) of the anions were made using tetrabutyl ammonium salt of the anions in acetonitrile, or the sodium salt in deionized water.

2.1. Computational method

All calculations in this work were carried out using GAUSSIAN 03 program package [54]. The Becke three parameters hybrid exchange [55] and the Lee-Yang-Parr correlation functionals [56] (B3LYP) were used. Geometry optimization of the studied molecules was carried out with the Density Functional Theory (DFT) method using 6-31G(d,p) basis set in vacuum. The obtained structure was optimized again using 3-21G* basis set in water using Polarized Continuum Model 3 (PCM). The optimized structure in water (used for later calculations) were done using higher basis set 6-31G(d,p). Time-Dependent Density Functional Theory (TD-DFT) [57,58], using 6-31G(d,p) basis set, was performed, in water, using the PCM model. The lowest 20 singlet-to-singlet spin-allowed excitation states were taken into account for TD-DFT calculations [59].

3. Results and discussion

3.1 UV-vis spectra of compound 1 in protic and in polar aprotic solvents

The aqueous solution of compound **1** (1.0×10^{-3} M) is yellow, while in acetonitrile is almost colorless. The presence of the yellow color is indicative of dissociation, resulting in a charge transfer band. This dissociation results in the formation of the phenolate ion **2** (Scheme 1), which is responsible for the observed color.

The UV-vis spectra of compound **1** were recorded in acetonitrile, water:acetonitrile (*v*:*v*, 1:9) and water solutions. The spectra showed a band at 298 nm in acetonitrile while in aqueous media it shifts to 314 nm, and an additional band appears at 387 nm associated with solvent effect. This red shift of the 298 nm peak indicates that it originates from $n \rightarrow \pi^*$ transition. These results are presented in Figure 1.

The dissociation was also detected in the NMR spectra of the compound in organic solvents and in D_2O. In acetonitrile-d_3, $CDCl_3$ or DMSO-d_6, a well-defined spectrum with very distinct peaks that represent the compound, were observed. Upon addition of D_2O the solution turns yellow and a complex spectrum is obtained in both ^{1}H- and ^{13}C-NMR. This indicates the formation of a new species constituting 17% of the mixture.

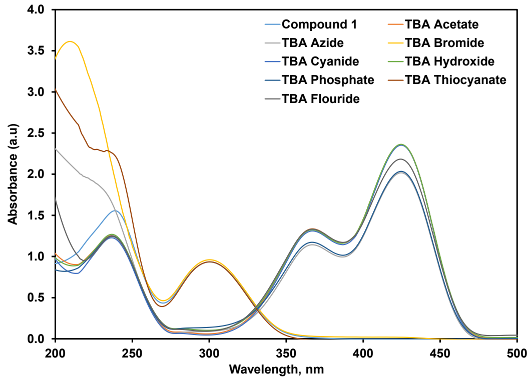

Figure 2. UV-vis spectra of compound **1** (1.0×10^{-4} M) in acetonitrile with various TBA salts of the anions (3 equivalents).

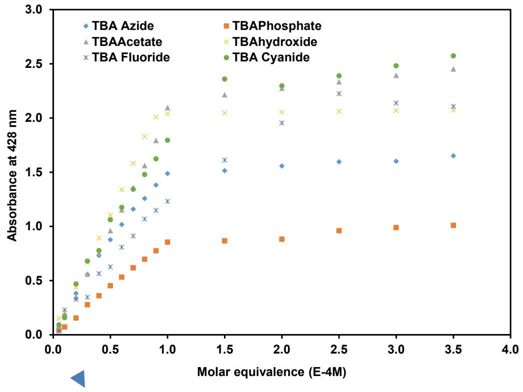

Figure 3. UV-vis spectra for titration of compound **1** (1.0×10^{-4} M) in acetonitrile with incremental increase of various TBA anions in acetonitrile at 425 nm.

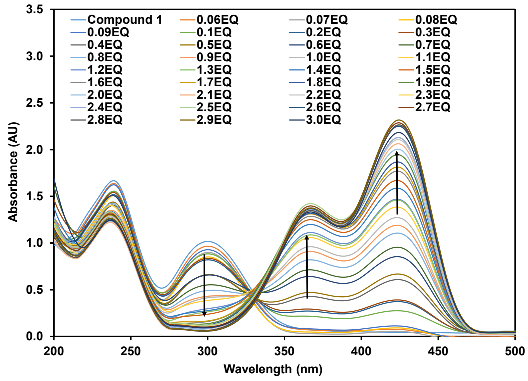

Figure 4. UV-Vis spectral changes of compound **1** (1.0×10^{-4} M) in CH_3CN, upon the addition of 0-3 equivalents of F^-.

3.2 Titration of compound 1with various anions in acetonitrile

UV-Vis spectra of (1.0×10^{-4} M) of compound **1** in the presence of 3 equivalents of cyanide, acetate, dihydrogen phosphate (DHP), fluoride, chloride, bromide, azide, perchlorate and hydrogen sulfate as their tetrabutyl ammonium salt were recorded. The results are shown in Figure 2. As obviously seen, cyanide, fluoride, acetate, dihydrogen phosphate anions selectively cause dramatic effects on the spectrum of compound **1** with the appearance of two bands at 368 and 425 nm and the diminishing intensity of the band at 298 nm. Other anions did not show any significant color or spectral change.

Titrations of compound **1** with varying amounts of anions were performed. A direct relationship was noticed between the intensity of the bands at 368 and 425 nm, and the added amount of interacting anions. The absorption plateaued upon addition of 1 equivalent of cyanide and acetate, while 2 and 3 equivalents for fluoride and dihydrogen phosphate were needed, respectively, Figure 3.

The titration curves with fluoride, cyanide, acetate, dihydrogen phosphates are presented in Figures 4-7, respectively. An isosbestic point is observed at 330 nm indicating the formation of a complex.

3.3. Stoichiometry and binding constants

The stoichiometry in the complex was obtained by Job plots for a total concentration of sensor and anion as 1.0×10^{-4} M. The job plots were performed and showed 1:1 stoichiometry for cyanide, hydroxide, fluoride, acetate and 2:1 for DHP.

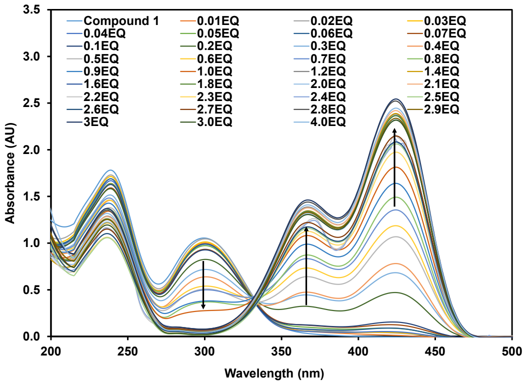

Figure 5. UV-Vis spectral changes of compound **1** (1.0×10^{-4} M) in CH_3CN upon the addition of 0-3 equivalence of CN^-.

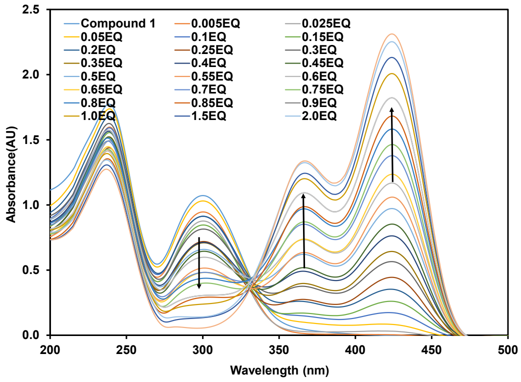

Figure 6. UV-Vis spectral changes of compound **1** (1×10^{-4} M) in CH_3CN upon the addition of 0-3 equivalents of AcO^-

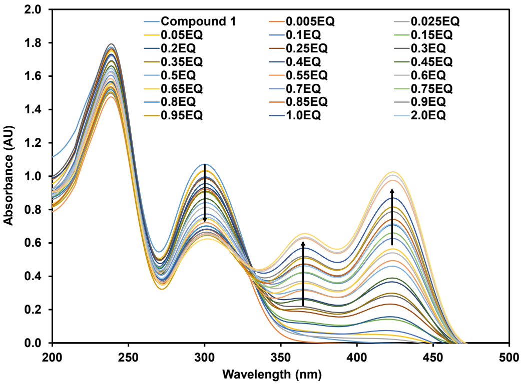

Figure 7. UV-Vis spectral changes of compound **1** (1.0×10^{-4} M) in CH_3CN, upon the addition of 0-3.5 equivalents of $H_2PO_4^-$.

The stoichiometry for DHP may be explained based on dimerization to $H_3P_2O_7^-$ [45,60]. The binding constants (K) were obtained according to Benesi-Hildebrand method, K = $4.5\times10^{3}\pm1.73\times10^{1,}$ K = $1.7\times10^{3}\pm49$, K = $3.2\times10^{3}\pm81$, K = $3.2\times10^{3}\pm81$ for cyanide, hydroxide, acetate, fluoride, DHP, respectively.

3.4. Titrations of compound 1 in water

The selectivity in acetonitrile, observed with non-basic anions, is attributed to hydrogen bonding. The interaction is diminished upon addition of water that competes for the anions and forms hydrogen bonding, indicated by color fading. Such phenomenon was utilized to enhance the selectivity towards cyanide. Cyanide is highly nucleophilic in water, so it interacts strongly with the probe to give a distinguished color change. Hydroxide ion (being a strong base) deprotonated the probe giving similar color and spectral changes. Acetate with lower basicity exhibited moderate to weak interaction. Indeed, the titration experiments in water showed such trend. The interaction of these anions in water, the spectral changes are presented in Figure 8 and the effect of tested ions is demonstrated in Figure 9.

The interaction of cyanide is expected to be due to nucleophilic addition to the aldehyde carbonyl, followed by an intramolecular proton transfer from the phenolic oxygen to give cyanohydrin compound **3**, as presented in Scheme 2. This in turn would lead to charge transfer, and more intense color, thus to the described spectral changes (*vide supra*). The UV-Vis absorption plots with varying amounts of added anions are shown in Figure 10.

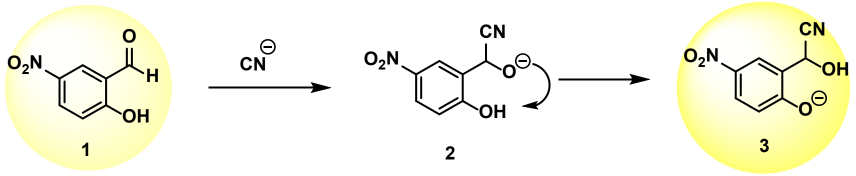

Scheme 2. Mechanism of addition of cyanide to form the cyanohydrin conjugate base.

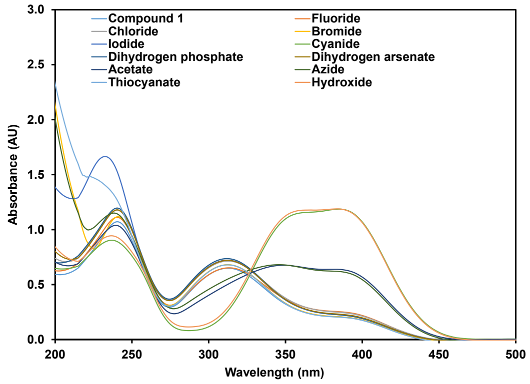

Figure 8. The UV-Vis spectra of compound **1** (1×10^{-4} M) in aqueous solution with the presence of different anions (3 equivalents).

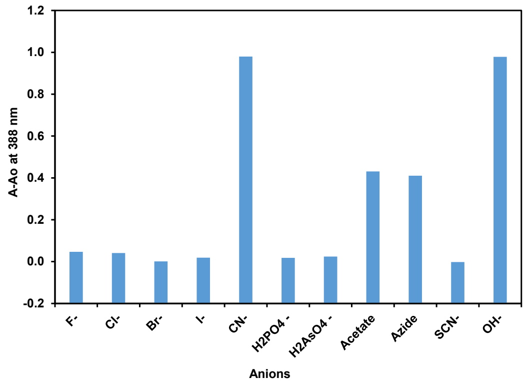

Figure 9. Bar graph of absorbance intensity change at 388 nm of 1.0×10^{-4} M compound **1** in water in the presence of 3 equivalents of indicated anions.

The interaction with cyanide and hydroxide caused an increase in the intensity of color and the absorption bands at 358 and 387 nm, and a decrease in that of the peak at 314 nm, with both cyanide and hydroxide ions.

The formation of the phenolate is confirmed by NMR studies that clearly demonstrate the structural changes in compound **1** upon addition of cyanide. The formation of cyanohydrin is clearly confirmed by the appearance of a peak at δ 5.67 ppm in ^{1}H NMR (C*H*OHCN) and disappearance of the aldehyde proton at δ 10.02 ppm [61]. The phenoxide formation is indicated by the up-field shift of the aromatic hydrogens due to shielding effect of the negative charge in addition to the disappearance of the phenolic proton. Again, a dramatic effect was observed in the ^{13}C NMR by the appearance of a signal at δ 60.02 ppm for the cyanohydrin carbon and decrease of the aldehyde carbonyl carbon at δ 193.14 ppm and up-field shifting of the aromatic carbons.

On the other hand, hydrogen sulfate caused the peaks at 368 and 387 nm to decrease in the UV-vis spectrum, while that at 314 nm to increase. This is due to protonation of the phenolate anion and the shift in the equilibrium to the left in Scheme 1.

3.5. Titration of compound 1 with sodium cyanide, sodium hydroxide in water

A solution of 1.0×10^{-4} M of compound **1** in water was titrated with varying amounts of sodium cyanide. The UV-vis spectra are presented in Figure 11.

Titration of compound **1** with varying concentration of sodium hydroxide and acetate in water gave results analogous to that of cyanide. This supports the mechanism proposed for cyanide (presented in Scheme 2) that resulted in a gradual hyper-chromic shift of the band at 387 nm. These results are depicted in Figure 11. The binding constants of the significant ions respectively are $K = 3.19\times10^3\pm25$, $K = 3.69\times10^3\pm413$, $K = 2.56\times10^3\pm250$ for hydroxide, cyanide and acetate. Cyanide presents the highest binding constant and a stoichiometry of 1:1 as deduced from Job's plot in Figure 12. The lower detection limit for cyanide was found to be 0.51 μM in acetonitrile and 1.45 μM in water.

Compound **1** showed no color or significant spectral changes in aqueous solutions in the presence of fluoride or DHP ions, as water eliminates the effect of hydrogen bonding in the interaction.

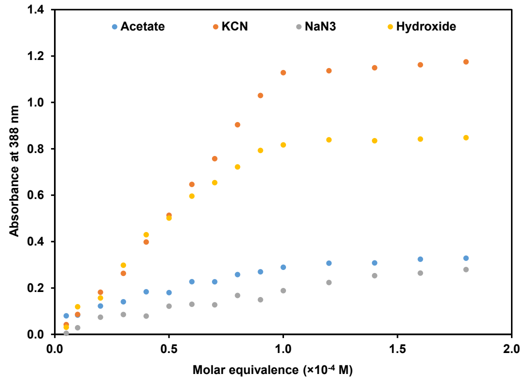

Figure 10. Titration of 1.0×10^{-4} M of compound **1** in water with incremental increase of various anions at 388 nm.

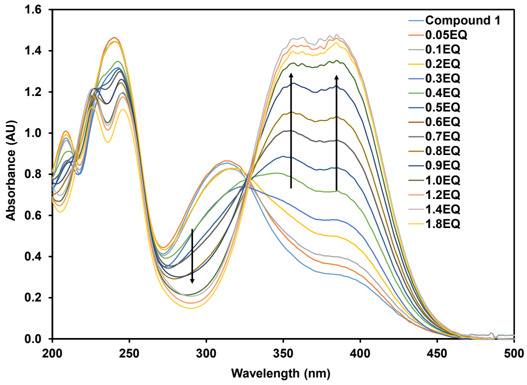

Figure 11. The UV-Vis spectra of compound **1** (1.0×10^{-4} M) in aqueous solution upon titration with cyanide (0.0-1.8 equivalents, 0.1 increments).

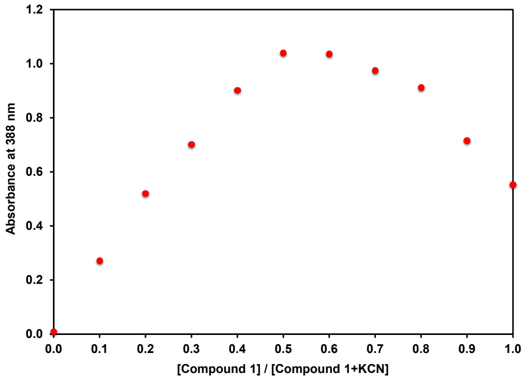

Figure 12. Job’s plot of compound **1** in the presence of cyanide in aqueous solution.

Hydrogen sulfate causes the yellow color of the solution to fade and the band at 387 nm to decrease and the absorption at 314 to increase

3.6. Theoretical calculations

DFT and TD-DFT calculations, in water, were performed for the three molecules; the phenol compound **1**, the phenolate anion **2** and the corresponding cyanohydrin conjugate base **3**. Molecular Orbitals (MOs) energy values for the species are presented in Table 1, and the corresponding energy levels diagrams for MOs are shown in Figure 13. Expected spectrum from theoretical calculations is shown in Figure 14. Calculation results found that the HOMO-LUMO (H-L) energy gaps for the phenol and phenolate forms are around 4.03 and 3.55 eV, respectively. This explains the red shift observed experimenttally by UV-Vis spectroscopy upon deprotonation of the phenol form. Similar observations were found for the cyanohydrin conjugate base **3**, which has an energy gap, around 3.26 eV. It is obvious that the molecular orbitals of compound **3** are different from those for compound **2**, in some cases the difference is very large, like the ones between L+1 and L+3 orbitals. However the difference is minimal for HOMO π-orbital which might indicate that CN group is not contributing significantly to the orbital. To create a better picture about the absorption spectrum of the studied molecules and the effect of nucleophilic addition of CN group to the aldehyde carbonyl, the TD-DFT calculations were performed for the three molecules in water using PCM model. Keeping into consideration that the PCM model is simulating the solvent as a dielectric continuum and, therefore, only solvent-solute non-specific interactions are considered. Thus, difference between experiment and theory should be expected since specific

Table 1. Energy values of MOs in eV obtained by DFT calculations in water.

Molecular orbital	Compound 1 (Phenol)	Compound 2 (Phenolate)	Compound 3 (-CN Phenolate)
L+3	+0.89	+1.85	+1.19
L+2	-0.10	+0.92	+0.81
L+1	-2.11	-1.08	-0.32
L	-2.95	-1.85	-2.09
H	-6.98	-5.40	-5.35
H-1	-7.26	-5.78	-6.11
H-2	-7.68	-6.83	-7.03
H-3	-8.14	-7.05	-7.17

Table 2. Computed excitation energies, and transition oscillator strengths (f) (transitions with wavelength > 250 nm just listed).

Compound 1		Compound 2		Compound 3	
λ (nm)	*F*	λ (nm)	*F*	λ (nm)	*F*
359.7	0	399.9	0	403.4	0.0021
347.4	0	364.1	0.3677	364.9	0.5578
335.4	0	363.8	0.0124	351.2	0.0006
333.1	0.3117	322.3	0	299.6	0.0002
314.6	0.0269	316.6	0.2045	297.6	0.0023
310.3	0.0001	292.9	0	286.0	0.0725
286.1	0.1249	277.1	0.0184	261.4	0.0009
		275.2	0.0001		
		267.4	0		

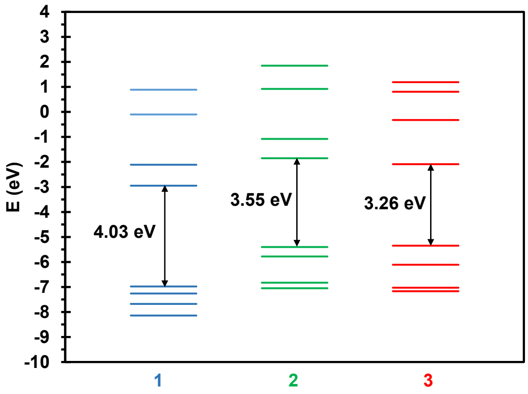

Figure 13. MO energy diagram for the studied molecules.

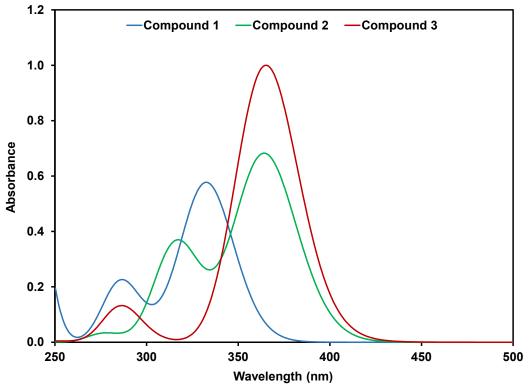

Figure 14. Expected (via theoretical calculations) spectrum for compounds **1**-**3** defined in text.

solvent-solute interactions are important when dealing with water as solvent.

Electronic absorption spectra of molecules **1**, **2** and **3**, were computed using TD-DFT calculations. The lowest 20 singlet-to-singlet spin-allowed excitation states in water were taken into account for the calculations of the electronic absorption spectrum for the optimized molecules via TD-DFT method using 6-31G(d,p). The calculated energy of excitation states and transition oscillator strength (*f*) are shown in Table 2. The absorption spectra of compounds **1**, **2** and **3** were simulated using GaussSum software based on the obtained TD-DFT results. Each excited state was interpolated by a Gaussian convolution with the full width at half-maximum (FWHM) of 3000 cm^{-1}. Figure 14 shows that the simulated spectra of the studied molecules. TD-DFT calculations show that the broad band centered at 314 nm (experimental) (calculated: 334 nm) for compound **1** shows a red shift to around 366 nm (calculated) upon deprotonation of compound **2**. Approximately, the same shift was observed for the cyanohydrin **3**. This red shift is in accordance with the experiment (Figure 8). It is interesting to note that the position of the peak in the red region of the spectrum is the same for compounds **2** and **3**.

This is also in agreement with the experimental findings. However, the experimentally observed spectrum Figure 8 reveals the splitting of peak for both molecules, a result that was not obtained by the present calculations. Examining the excitation energies presented in Table 2 reveals the existence of transitions occurring at around 400 nm for compound **2** and **3** but with low or zero oscillator strength and hence were not contributing significantly to the simulated spectrum. It should be noted here that the oscillator strength is very sensitive to basis set error or solvent effect, which may be the reason behind underestimating the oscillator strength for transition around 400 nm. This also can be seen in the unequal intensity of the peak around 366 nm (calculated) for compound **1** and **2** whereas similar intensities were obtained experimentally.

4. Conclusion

5-Nitro-salicylaldehyde proved to be selective, sensitive anion sensor. It is sensitive and selective to fluoride, cyanide, acetate, and dihydrogen phosphate in organic solvents such as acetonitrile with a stoichiometry of 1:1. Compound **1** is highly selective to cyanide as chemodosimeter in pure water solution. Theoretical calculations were in agreement with the experimental results

Acknowledgments

This work was supported National Priority Research Program (NPRP) award [NPRP-7-495-01-094] from the Qatar National Research Fund (a member of The Qatar Foundation). The statements made herein are solely the responsibility of the authors.

Disclosure statement

Conflict of interests: The authors declare that they have no conflict of interest.
Author contributions: All authors contributed equally to this work.
Ethical approval: All ethical guidelines have been adhered.
Sample availability: Samples of the compounds are available from the author.

Funding

Qatar National Research Fund
http://dx.doi.org/10.13039/100008982

ORCID

Yousef Mohammad Hijji
http://orcid.org/0000-0002-4116-1746
Hani Darwish Tabba
http://orcid.org/0000-0002-5313-6951
Rajeesha Rajan
http://orcid.org/0000-0002-8798-8992
Hamzeh Mohammad Abdel-Halim
http://orcid.org/0000-0003-0564-7922
Musa Ibrahim El-Barghouthi
http://orcid.org/0000-0003-1961-796X
Hutaf Mustafa Baker
http://orcid.org/0000-0002-0690-0726

References

[1]. Gotor, R.; Costero, A. M.; Gil, S.; Parra, M.; Martinez-Manez, R.; Sancenon, F. *Chem. A Eur. J.* **2011**, *17*, 11994-11997.
[2]. Sun, W.; Guo, S.; Hu, C.; Fan, J.; Peng, X. *Chem. Rev.* **2016**, *116*, 7768-7817.
[3]. Moragues, M. E.; Martinez-Manez, R.; Sancenon, F. *Chem. Soc. Rev.* **2011**, *40*, 2593-2643.
[4]. Zang, L.; Wei, D.; Wang, S.; Jiang, S. *Tetrahedron* **2012**, *68*, 636-641.
[5]. Sun, Y.; Wang, G.; Guo, W. *Tetrahedron* **2009**, *65*, 3480-3485.
[6]. Duke, R. M.; Veale, E. B.; Pfeffer, F. M.; Kruger, P. E.; Gunnlaugsson, T. *Chem. Soc. Rev.* **2010**, *39*, 3936-3953.
[7]. Garcia, J. M.; Garcia, F. C.; Serna, F.; De La Pena, J. L. *Polymer Rev.* **2011**, *51*, 341-390.
[8]. Gunnlaugsson, T.; Glynn, M.; Tocci, G. M.; Kruger, P. E.; Pfeffer, F. M. *Coord. Chem. Rev.* **2006**, *250*, 3094-3117.
[9]. Chang, K. C.; Sun, S. S.; Odago, M. O.; Lees, A. J. *Coord. Chem. Rev.* **2015**, *284*, 111-123.
[10]. Wu, J.; Kwon, B.; Liu, W.; Anslyn, E. V.; Wang, P.; Kim, J. S. *Chem. Rev.* **2015**, *115(15) 7893-7943.*
[11]. Udhayakumari, D. *Sensors Actuators B: Chem.* **2018**, *259*, 1022-1057.
[12]. Bhattacharya, R.; Flora, S. J. S. In Handbook of Toxicology of Chemical Warfare Agents (Second Edition); Gupta, R. C., Ed.; Academic Press: Boston, 2015, 301-314.
[13]. Gilley, C.; MacDonald, M.; Nachon, F.; Schopfer, L. M.; Zhang, J.; Cashman, J. R.; Lockridge, O. *Chem. Res. Toxicol.* **2009**, *22*, 1680-1688.
[14]. Rhee, J.; Jung, J.; Yeom, H.; Lee, H.; Lee, S.; Park, Y.; Chung, H. *Forensic Sci. Inter.* **2011**, *210*, e12-e15.
[15]. Xu, Z.; Chen, X.; Kim, H. N.; Yoon, J. *Chem. Soc. Rev.* **2010**, *39*, 127-137.
[16]. Hijji, Y. M.; Barare, B.; Kennedy, A. P.; Butcher, R. *Sensors Actuators B: Chem.* **2009**, *136*, 297-302.
[17]. Odago, M. O.; Colabello, D. M.; Lees, A. J. *Tetrahedron* **2010**, *66*, 7465-7471.
[18]. Jo, H. Y.; Lee, S. A.; Na, Y. J.; Park, G. J.; Kim, C. *Inorg. Chem. Commun.* **2015**, *54*, 73-76.
[19]. Elsafy, A.; Al-Easa, H.; Hijji, Y. *Sensors* **2018**, *18*, 2219-2230.
[20]. Wei, T.; Li, H.; Wang, Q.; Yan, G.; Zhu, Y.; Lu, T.; Shi, B.; Lin, Q.; Zhang, Y. *Supramol. Chem.* **2016**, *28*, 314-320.
[21]. Lee, E. M.; Gwon, S. Y.; Son, Y. A.; Kim, S. H. *Spectrochim. Acta A* **2012**, *95*, 25-28.
[22]. Yu, Y.; Shu, T.; Yu, B.; Deng, Y.; Fu, C.; Gao, Y.; Dong, C.; Ruan, Y. *Sensors Actuators B: Chem.* **2018**, *255*, 3170-3178.
[23]. Zhou, C.; Sun, M.; Yan, C.; Yang, Q.; Li, Y.; Song, Y. *Sensors Actuators B: Chem.* **2014**, *203*, 382-387.
[24]. Lou, X.; Ou, D.; Li, Q.; Li, Z. *Chem. Commun.* **2012**, *48*, 8462-8477.
[25]. Tang, Y. H.; Qu, Y.; Song, Z.; He, X. P.; Xie, J.; Hua, J.; Chen, G. R. *Org. Biomol. Chem.* **2012**, *10*, 555-560.
[26]. Jung, H. S.; Han, J. H.; Kim, Z. H.; Kang, C.; Kim, J. S. *Org. Lett.* **2011**, *13*, 5056-5059.
[27]. Chen, H.; Liu, Z.; Cao, D.; Lu, S.; Pang, J.; Sun, Y. *Sensors Actuators B: Chem.* **2014**, *199*, 115-120.
[28]. Isaad, J.; El Achari, A. *Tetrahedron* **2011**, *67*, 4939-4947.
[29]. Lee, J. H.; Jeong, A. R.; Shin, I. S.; Kim, H. J.; Hong, J. I. *Org. Lett.* **2010**, *12*, 764-767.
[30]. Dong, X.; Zhou, Y.; Song, Y.; Qu, J. *J. Fluor. Chem.* **2015**, *178*, 61-67.
[31]. Dong, Y. M.; Peng, Y.; Dong, M.; Wang, Y. W. *J. Org. Chem.* **2011**, *76*, 6962-6966.
[32]. Lin, Y. D.; Peng, Y. S.; Su, W.; Tu, C. H.; Sun, C. H.; Chow, T. J. *Tetrahedron* **2012**, *68*, 2523-2526.
[33]. Park, S.; Kim, H. J. *Sensors Actuators B: Chem.* **2012**, *161*, 317-321.
[34]. Fu, G. L.; Zhao, C. H. *Tetrahedron* **2013**, *69*, 1700-1704.
[35]. Niamnont, N.; Khumsri, A.; Promchat, A.; Tumcharern, G.; Sukwattanasinitt, M. *J. Hazard. Mater.* **2014**, *280*, 458-463.
[36]. Bejoymohandas, K. S.; Kumar, A.; Sreenadh, S.; Varathan, E.; Varughese, S.; Subramanian, V.; Reddy, M. L. P. *Inorg. Chem.* **2016**, *55*, 3448-3461.
[37]. Huo, F.; Zhang, Y.; Yue, Y.; Chao, J.; Zhang, Y.; Yin, C. *Dyes Pigments* **2017**, *143*, 270-275.
[38]. Kim, D. S.; Chung, Y. M.; Jun, M.; Ahn, K. H. *J. Org. Chem.* **2009**, *74*, 4849-4854.
[39]. Isaad, J.; Perwuelz, A. *Tetrahedron Lett.* **2010**, *51*, 5810-5814.
[40]. Ding, Y.; Li, T.; Zhu, W.; Xie, Y. *Org. Biomol. Chem.* **2012**, *10*, 4201-4207.
[41]. Isaad, J.; Achari, A. E. *Anal. Chim. Acta* **2011**, *694*, 120-127.
[42]. Isaad, J.; El Achari, A. *Tetrahedron* **2011**, *67*, 4196-4201.
[43]. Goswami, S.; Manna, A.; Paul, S.; Aich, K.; Das, A. K.; Chakraborty, S. *Tetrahedron Lett.* **2013**, *54*, 1785-1789.
[44]. Saravanakumar, D.; Devaraj, S.; Iyyampillai, S.; Mohandoss, K.; Kandaswamy, M. *Tetrahedron Lett.* **2008**, *49*, 127-132.
[45]. Hijji, Y. M.; Barare, B.; Zhang, Y. *Sensors Actuators, B: Chem.* **2012**, *169*, 106-112.
[46]. Kumar, S.; Singh, P.; Hundal, G.; Singh Hundal, M. *Chem. Commun.* **2013**, *49*, 2667-2669.
[47]. Lin, Y. S.; Zheng, J. X.; Tsui, Y. K.; Yen, Y. P. *Spectrochim. Acta A* **2011**, *79*, 1552-1558.
[48]. Kang, J.; Song, E. J.; Kim, H.; Kim, Y. H.; Kim, Y.; Kim, S. J.; Kim, C. *Tetrahedron Lett.* **2013**, *54*, 1015-1019.
[49]. Niu, H. T.; Su, D.; Jiang, X.; Yang, W.; Yin, Z.; He, J.; Cheng, J. P. *Org. Biomol. Chem.* **2008**, *6*, 3038-3040.
[50]. Jang, H. J.; Kang, J. H.; Lee, M.; Lim, M. H.; Kim, C. *Ind. Eng. Chem. Res.* **2018**, *57*, 54-62.
[51]. Li, H.; Li, B.; Jin, L. Y.; Kan, Y.; Yin, B. *Tetrahedron* **2011**, *67*, 7348-7353.

[52]. Yang, Y. K.; Tae, J. *Organic Lett.* **2006**, *8*, 5721-5723.

[53]. Guo, Y. Y.; Tang, X. L.; Hou, F. P.; Wu, J.; Dou, W.; Qin, W. W.; Ru, J. X.; Zhang, G. L.; Liu, W. S.; Yao, X. J. *Sensors Actuators B: Chem.* **2013**, *181*, 202-208.

[54]. Gaussian 03. Frisch, M. J.; Trucks, G. W.; Schlegel, H. B.; Scuseria, G. E.; Robb, M. A.; Cheeseman, J. R.; Montgomery, J. A. Jr.; Vreven, T.; Kudin, K. N.; Burant, J. C.; Millam, J. M.; Iyengar, S. S.; Tomasi, J.; Barone, V.; Mennucci, B.; Cossi, M.; Scalmani, G.; Rega, N.;. Petersson, G. A.; Nakatsuji, H.; Hada, M.; Ehara, M.; Toyota, K.; Fukuda, R.; Hasegawa, J.; Ishida, M.; Nakajima, T.; Honda, Y.; Kitao, O.; Nakai, H.; Klene, M.; Li, X.; Knox, J. E.; Hratchian, H. P.; Cross, J. B.; Adamo, C.; Jaramillo, J.; Gomperts, R.; Stratmann, R. E.; Yazyev, O.; Austin, A. J.; Cammi, R.; Pomelli, C.; Ochterski, J. W.; Ayala, P. Y.; Morokuma, K.; Voth, G. A.; Salvador, P.; Dannenberg, J. J.; Zakrzewski, V. G.; Dapprich, S.; Daniels, A. D.; Strain, M. C.; Farkas, O.; Malick, D. K.; Rabuck, A. D.; Raghavachari, K.; Foresman, J. B.; Ortiz, J. V.; Cui, Q.; Baboul, A. G.; Clifford, S.; Cioslowski, J.; Stefanov, B. B.; Liu, G.; Liashenko, A.; Piskorz, P.; Komaromi, I.; Martin, R. L.; Fox, D. J.; Keith, T. Al-Laham, M. A.; Peng, C. Y.; Nanayakkara, A.; Challacombe, M.; Gill, P. M. W.; Johnson, B.; Chen, W.; Wong, M. W.; Gonzalez, C.; Pople, J. A. Gaussian, Inc., Pittsburgh PA, 2003.

[55]. Becke, A. D. *J. Chem. Phys.* **1993**, *98*, 5648-5652.

[56]. Lee, C.; Yang, W.; Parr, R. G. *Physical Rev. B* **1988**, *37*, 785-789.

[57]. Runge, E.; Gross, E. K. U. *Phys. Rev. Lett.* **1984**, *52*, 997-1000.

[58]. Casida, M. K.; Chong, D. P., Ed.; Recent advances in density and functional methods , World Scientific, Singapore 1995; Vol. 1, pp. 155-192.

[59]. O'Boyle, N. M.; Tenderholt, A. L.; Langner, K. M. *J. Comp. Chem.* **2008**, *29*, 839-645.

[60]. Jana, S.; Dalapati, S.; Alam, M. A.; Guchhait, N. *Spectrochim. Acta A* **2012**, *92*, 131-136.

[61]. Pati, P. B.; Zade, S. S. *Eur. J. Org. Chem.* **2012**, *2012*, 6555-6561.